Title

The role of metabolic imaging in radiation therapy of prostate cancer

Journal

NMR in Biomedicine, 27(1)

ISSN

0952-3480

Authors

Zhang, VY
Westphalen, A
Santos, L Delos
et al.

Publication Date

2014

DOI

10.1002/nbm.3007

Peer reviewed

Published in final edited form as:
NMR Biomed. 2014 January ; 27(1): . doi:10.1002/nbm.3007.

The Role of Metabolic Imaging in Radiation Therapy of Prostate Cancer

V. Y. Zhang[1], **A. Westphalen**[1], **L. Delos Santos**[1], **Z.L. Tabatabai**[2], **K. Shinohara**[3], **D.B. Vigneron**[1], and **J. Kurhanewicz**[1]

[1]Department of Radiology and Biomedical Imaging, University of California San Francisco (UCSF), California, United States

[2]Department of Pathology, University of California San Francisco (UCSF), California, United States

[3]Department of Urology, University of California San Francisco (UCSF), California, United States

Abstract

The goal of this study was to correlate prostatic metabolite concentrations from snap-frozen patient biopsies of recurrent cancer after failed radiation therapy with histopathological findings, including Ki-67 immunohistochemistry and pathologic grade, in order to identify quantitative metabolic biomarkers that predict for residual aggressive *versus* indolent cancer. A total of 124 snap-frozen transrectal ultrasound (TRUS) – guided biopsies were acquired from 47 men with untreated prostate cancer and from 39 men with a rising PSA and recurrent prostate cancer following radiation therapy. Biopsy tissues with Ki-67 labeling index ≤ 5% were classified as indolent cancer, while biopsy tissues with Ki-67 labeling index > 5% were classified as aggressive cancer. The majority (15 out of 17) of cancers classified as aggressive had a primary Gleason 4 pattern (Gleason score ≥ 4+3). The concentrations of choline – containing phospholipid metabolites (PC, GPC and free Cho), and lactate were significantly elevated in recurrent cancer relative to surrounding benign tissues. There was also a significant increase in [PC] and reduction in [GPC] concentration between untreated and irradiated prostate cancer biopsies. The concentration of the choline containing phospholipid metabolites was significantly higher in recurrent aggressive (≈ 2 fold) than in recurrent indolent cancer biopsies, and the receiver operating characteristic (ROC) curve analysis of total choline to creatine ratio (tCho/Cr) demonstrated an accuracy of 95% (confidence interval = 0.88 to 1.00) for predicting aggressive recurrent disease. The tCho/Cr was significantly higher for identifying recurrent aggressive *versus* indolent cancer (tCho/Cr = 2.4 ± 0.4 *versus* 1.5 ± 0.2) suggesting that use of a higher threshold tCho/Cr ratio in future *in vivo* ^{1}H MRSI studies could improve the selection and therapeutic planning of patients that would benefit most from salvage focal therapy after failed radiation therapy.

Keywords

Radiation therapy; Phospholipid Metabolism; Prostate Cancer; Pathologic grade; Gleason score; Ki-67; HR-MAS; MR spectroscopy

*Correspondence and Reprint Request: Prof. John Kurhanewicz, UCSF Mission Bay Campus, Byers Hall, Room 203E, 1700 4th St, San Francisco, CA 94158-2330, Tel: (415) 514-9711, Fax: (415) 514-9656.

INTRODUCTION

An estimated 241,740 men will be diagnosed with prostate cancer in the United States in 2012 (1) and many of these men will be treated with external beam radiation therapy (2). Approximately half of these patients are expected to develop biochemical failure, i.e. a rising serum prostate-specific antigen (PSA) after a post-treatment nadir has been reached (3), which triggers investigation for the presence of recurrent local and/or metastatic disease. The diagnosis of locally recurrent prostate cancer after radiation therapy is largely dependent on histopathology obtained from transrectal ultrasound (TRUS) – guided prostate biopsies. TRUS localizes the prostate, however often does not visualize the malignant focus well because 37% to 50% of cancers may be isoechoic or only slightly hypoechoic (4). Accordingly, TRUS-guided biopsy has demonstrated false negative rates of up to 30% (5). Post-radiation prostate biopsies are also prone to problems in pathologic interpretation due to radiation effects confounding assessments of the presence, aggressiveness and viability of the residual tumor (6–8). The diagnosis of recurrent cancer after radiation therapy is further hindered by the long time to reach a PSA nadir after treatment, a process that can take up to 24 months (9,10).

Endorectal magnetic resonance (MR) imaging allows for an assessment of the entire prostate. However, T_2-weighted MR imaging of the irradiated prostate is limited by the post-treatment loss of zonal anatomy and diffuse low signal, which hinders tumor detection (11–14) (Figure 1A). Proton MR spectroscopic imaging (^{1}H MRSI) diagnoses of prostate cancer is based on the identification of neoplastic metabolism (15,16) and studies have demonstrated the ability of combined MRI/^{1}H MRSI to discriminate residual or recurrent prostate cancer from residual benign tissue and atrophic/necrotic tissue after radiation therapy (17,18) (Figure 1C, D). These studies have relied on elevated choline to creatine as a metabolic marker for residual prostate cancer presence since the prostate metabolites polyamines and citrate, which are present in prostate tissue prior to therapy, are reduced to undetectable levels early after radiation therapy in both post-radiated benign and malignant tissues (17,18). Two published MRI/^{1}H MRSI studies of prostate cancer patients after radiation therapy have demonstrated that three or more consecutive spectroscopic voxels having total choline/creatine >1.5 resulted in the ability to predict the presence of cancer after radiation therapy with an accuracy of ≈ 80% (11,19) (Figure 1C, D). Moreover, the addition of MR spectroscopic imaging to T_2-weighted MR imaging (area under the receiver operating characteristic curve or AUC = 0.79) was shown to significantly improve the diagnostic accuracy of T_2-weighted MR imaging alone (AUC = 0.67) in the detection of locally recurrent prostate cancer after definitive external beam radiation therapy (19). Alternatively, the lack of metabolic evidence of locally recurrent cancer after radiation therapy predicts for effective local treatment. This in the face of a rising serum PSA triggers concern for the presence of metastatic disease, thereby changing therapeutic intervention from a focal to a systemic approach.

It has also been shown that exposure of tumors to radiotherapy consistently lead to measurable increases in water diffusion in cases of favorable treatment response, however regions of cancer still remained lower than surrounding benign and atrophic tissues (Figure 1B) (20,21). After radiation therapy, the mean apparent diffusion coefficient (ADC) values of the biopsy-proven cancer areas ($0.98 \pm 0.23 \times 10^{-3}$ mm^2/sec) were shown to be significantly lower than those of benign tissue ($1.60 \pm 0.21 \times 10^{-3}$ mm^2/sec (20). A significantly greater area under the ROC curve was determined for combined T_2 MRI and diffusion weighted imaging, or DWI (AUC = 0.88, $P < 0.01$) as compared to T_2 MRI alone (AUC = 0.61) (20). In another study, incorporation of ^{1}H MRSI to T_2-weighted (AUC = 0.84) and/or diffusion-weighted MRI (AUC = 0.86) significantly improved the assessment of patients with suspected recurrence after radiotherapy and a combined approach with all

three modalities (AUC = 0.87) may have the best diagnostic performance (21). Similar results were obtained by Haider et al. investigating the diagnostic value of dynamic contrast-enhanced (DCE) MR imaging after radiation therapy (22). Specifically, on a sextant basis, peak enhancement on DCE MRI had significantly better sensitivity (72% vs. 38%), positive predictive value (46% vs. 24%) and negative predictive value (95% *versus* 88% than T_2-weighted MRI for detecting residual disease after radiation therapy.

The non-invasive detection of residual/recurrent cancer at an early time following treatment using multiparametric MRI would have a significant clinical value by allowing earlier intervention with a number of possible salvage therapy approaches (23–27). However, because of long prostate cancer doubling times and the fact that radiation therapy causes post-mitotic cell death, histologic tumor clearance can be delayed, with 30% of patients with positive early biopsy findings demonstrating tumor resolution by 30 months after therapy (28). For the same reason, early ^{1}H MRSI findings positive for cancer often resolve themselves over time, with the mean time for metabolic resolution of prostate cancer being on the order of 24 to 40 months after radiation therapy depending on radiation dose (11,17,29). A recent study investigated early (within first eight weeks) changes of ADC coefficients and T_2 relaxation time and determined six weeks to be the optimum time point to detect radiation induced changes but the prediction of clinically progressive recurrent disease was not determined in this study (30). The selection of appropriate salvage therapy candidates early after radiation therapy requires the identification of aggressive/progressive *versus* indolent or dying prostate cancer.

The nuclear antigen, Ki-67, is present in proliferating cancer cells, and the presence of high Ki-67 staining has been associated with aggressive, high pathologic grade prostate cancer (31–33). Furthermore, >5% Ki-67 staining in post-radiation biopsy tissues has been associated with subsequent local failure (8,34,35) and the high likelihood of metastatic disease (32,33). In a *ex vivo* high resolution magic angle spinning (HR-MAS) spectroscopy study of surgically removed prostate tissues prior to therapy, Keshari et al. showed that proliferative, high-grade prostate cancers also have significantly higher concentrations of the choline-containing phospholipid metabolites, phosphocholine (PC) and glycerophosphocholine (GPC), than do low-grade prostate cancers and benign prostate tissues (36). This *ex vivo* finding is consistent with other *ex vivo* (37–42) and *in vivo* (43–46) ^{1}H spectroscopy studies, which have correlated the degree of elevation of the individual phospholipid metabolites and the composite *in vivo* choline resonance with cancer aggressiveness (Gleason grade). Recent studies have also identified other prostate metabolites, such as lactate and glutamate, as biomarkers of prostate cancer presence and aggressiveness (39,47,48). Based on these findings it is hypothesized that the identification of quantitative metabolic biomarkers of proliferative/aggressive locally recurrent cancer could improve the selection of patients that would benefit from salvage focal therapy and potentially improve the targeting of the focal therapy (49).

Accordingly, the goal of this study was to correlate metabolite concentrations from snap-frozen, patient biopsies of residual cancer after radiation therapy with histopathological findings, including pathologic grade and Ki-67 immunohistochemistry, to identify quantitative metabolic biomarkers that predict for residual aggressive *versus* indolent/dying cancer. These quantitative metabolic biomarkers will be used in future *in vivo* multiparametric MR studies to investigate the improvement they provide for the selection and therapeutic planning of patients that would benefit most from salvage focal therapy after failed radiation therapy.

Methods

Subjects

Our institutional research board reviewed and approved this study, it was compliant with United States Government Health Insurance Portability and Accountability Act (HIPAA) requirements, and informed consent was obtained from all patients.

A total of 124 TRUS-guided biopsy specimens acquired from 47 men with untreated prostate cancer and from 39 men with recurrent prostate cancer following radiation therapy were used for this study. The mean time interval from patient receiving radiation therapy administered to the prostate to TRUS-guided biopsy of the prostate was 6.4 years (range, 2 to 15 years). Detailed patient characteristics, including the types of radiation therapy received, are described in Table 1 and their biopsy characteristics are provided in Table 2.

Under TRUS-guidance, 16 to 20 core biopsy specimens were obtained as part of usual clinical care; two additional specimens were acquired for research purposes. These two specimens were immediately snap-frozen on dry ice in cryovials, and stored in −80°C until further analysis. Tessem MB et al. have detailed this process in a previous publication (48).

^{1}H HR-MAS Spectroscopy Acquisition

Acquired biopsy tissues (5.4±1.2 mg) were prepared as previously described (48), and placed into custom designed 20 μl or 35 μl leak proof zirconium rotors containing 3.0 μl deuterium oxide and 0.75 wt% sodium-3-trimethylsilylpropionate-2,2,3,3-d_4 acid (D_2O +TSP). Quantitative 1D ^{1}H HR-MAS ‘presat’ data were acquired at 11.7T (500 MHz for ^{1}H), 1°C, and 2,250 Hz spin rate using a Varian INOVA spectrometer, equipped with a 4 mm gHX nanoprobe (Varian Inc, Palo Alto). Fully relaxed water pre-saturated spectra were acquired using 40,000 points, 20,000-Hz spectral window, 2-s pre-saturation delay, 2-s acquisition time (total 4-s repetition time, or TR), four steady-state pulses, and 124 transients.

For quantification of prostate metabolites, an electronic reference was added using the electronic reference to access *in vivo* concentrations (ERETIC) method (50). The phase and amplitude of the ERETIC peak were chosen to match other peaks in the spectrum, and the signal was transmitted during acquisition using 0 dB of power, a full width at half height of 3.5 Hz, and an offset frequency equivalent to −0.5 ppm. The ERETIC signal was calibrated monthly using standard solution of D_2O + TSP.

2D total correlation spectroscopy (TOCSY) was acquired after the 1D ‘presat’ HR-MAS data acquisition. The TOCSY spectra were acquired using a rotor synchronized adiabatic (WURST-8) mixing scheme with 1-s pre-saturation delay, 0.2-s acquisition time, 40-ms mixing time, 24 transients/increment, 20,000 × 6000 Hz spectral width, 4096 × 64 complex points, and a time of ~1 hour (36,40).

^{1}H HR-MAS Spectroscopy Data Analysis and Quantification

Acquired HR-MAS biopsy data were processed offline using ACD/Labs 1D and 2D NMR processor version 9 (ACD/Labs, Toronto, Canada). 1D spectra were first prepared by linearly predicting the first two points of the FID. Each spectrum was phase – corrected, frequency – referenced to the CH_3 peak of creatine, and the residual water peak was removed using the Java-based graphical user interface for the Magnetic Resonance User Interface (jMRUI) package (51). 1D data were then quantified using the high resolution quantum estimation (HR-QUEST) method (52). To determine goodness of fit, HR-QUEST estimated the Cramér – Rao Lower Bounds (CRLB) percentages of the measured

metabolites for each prostate biopsy spectrum. Metabolites with CRLB >15% were excluded from analysis. By modeling the broad lipid and macromolecule resonance overlapping lactate at 1.33 ppm, HR-QUEST was able to resolve the lactate amplitude.

In 3 out of 53 biopsies, lactate measurements were considered unusable due to improper fit of the lipid and macromolecule peak at 1.33 ppm. Concentrations were calculated relative to the amplitude of the ERETIC signal according to Eq. [1]:

$$A_m = \frac{A_m}{A_e} \times [H_e] \times \frac{nH_e}{nH_m} \times \frac{1}{\text{Tissue mass}} = [M] \quad [1]$$

Where A_m = the metabolite amplitude, A_e = the amplitude of ERETIC signal, $[H_e]$ = the standard moles of protons associated with the ERETIC signal in mmol, nH_e = the number of protons of ERETIC (N = 1), nH_m = the number of protons corresponding to the main metabolite resonance used in HR-QUEST fitting, tissue mass = mass of the prostate biopsy (kg), and [M] = the metabolite concentration in mmolal.

2D TOCSY data were processed and quantified as described previously (36,40). PC and GPC concentrations were estimated using the side chain CH_2-CH_2 cross-peak volumes relative to the diagonal of TSP. PC, GPC and TSP cross-peaks were volume integrated and corrected for the magnetic transfer efficiency (K_{MT}). Concentrations were then calculated relative to the TSP cross-peak volume, TSP 1D integrated area and ERETIC 1D integrated area according to Eq. [2]:

$$\frac{V_{\text{met}}}{V_{\text{TSP}}} \times K_{\text{MT}} \times \frac{\text{Area}_{\text{TSP},1D}}{\text{Area}_e} \times [H_e] \times \frac{\text{nH}_e}{\text{nH}_m} \times \frac{1}{\text{Tissue mass}} = [M] \quad [2]$$

Where V_{met} = integrated volume of either PC or GPC cross-peak, V_{TSP} = integrated volume of the TSP diagonal peak, $Area_{TSP, 1D}$ = integrated area of the TSP peak from the 1D spectrum, $Area_e$ = integrated area of the ERETIC peak from the 1D spectrum.

Histopathologic Analysis

Following ^{1}H HR-MAS acquisition, biopsy tissues were frozen in Tissue-Tek® optimal cutting temperature (OCT) tissue – embedding medium (Fisher, Pittsburgh, PA, USA), and sectioned at −22°C using a Leica CM1850 cryostat (Leica Microsystem, Wetzlar, Germany). Tissues were sectioned at 5 to 7 μm intervals, placed on individual histology slides, and stained with hematoxylin and eosin (H&E) using a standard protocol. Additional sections were cut for high-molecular-weight keratin staining to confirm the presence of cancer, and Ki-67 immunohistochemical staining (53). For Ki-67, the slides were incubated for 60 min with a monoclonal mouse Ki-67 antibody, clone MIB-1 (M7240, Dako, Copenhagen, Denmark), diluted 1:100 at room temperature. Secondary antibody was peroxidase-labeled horseradish peroxidase polymer (Dako), incubated for 60 min. The antigen localization was achieved by the 3,3′-diaminobenzidine chromogen (Dako). Nuclei were considered to be Ki-67 positive if any nuclear staining was present, regardless of staining intensity.

Two pathologists (12 and 16 years of experience) reviewed the slides and estimated the percentage of benign glandular epithelium, stroma, prostatic intraepithelial neoplasia (PIN), benign prostatic hyperplasia (BPH), chronic inflammation (prostatitis), prostate cancer (Gleason grade), and % of Ki-67 positively stained tissue in each core. Benign prostatic biopsy tissues that consisted of ≥ 25% glandular tissue were defined as predominately glandular tissue. A Ki-67 labeling index was defined as the percentage of positively staining

cells for each cell type, as determined by counting approximately 1000 cells of that type. Pathology readings and Ki-67 labeling index were then recorded into a database and averaged for both readers. The malignant biopsy tissues were further separated according to their pathologic grade and Ki-67 labeling index. Biopsy tissues with Ki-67 labeling index ≤ 5% were classified as indolent cancer (8,34,35), while biopsy tissues with Ki-67 labeling index > 5% were classified as aggressive cancer (Table 2).

Statistical Analysis

Statistical analyses were performed using JMP Software (SAS Institute Inc., 2008, version 8.0). Metabolite concentrations (mmol/kg) were compared between benign and residual cancer tissues as well as among benign, indolent and aggressive residual cancer using a linear mixed-effects model (54). The model used metabolite concentrations as the dependent variable, disease status (Ki-67 labeling index and grade) as fixed effect and individual patients as random effect. Thus, effects from repeated samples of patients were removed. Non-parametric Wilcoxon Rank Sum Test or Kruskal-Wallis Test was used for multiple comparisons. For all statistical analyses, a probability value of less than 0.05 was considered significant. The performance of using total choline (PC + GPC + free choline) to creatine ratio to diagnose aggressive residual disease was described using receiver operating characteristic (ROC) curve. Biopsy tissues with Ki-67 staining greater than 5% were considered to be aggressive cancer (8).

Results

The average serum PSA level of patients with prostate cancer after therapy was significantly lower than prior to therapy, even for patients with similar amounts of recurrent cancer after therapy (Table 1). Figures 2 and 3 demonstrate representative ^{1}H HR-MAS spectra, H&E and Ki-67-stained histologic sections from benign, indolent and aggressive prostate cancer biopsies from patients prior to and after radiation therapy. Of the 71 untreated prostate biopsy specimens, histopathology demonstrated that 58 were benign tissues (38 predominately glandular, 20 predominately stromal), 5 were indolent cancers, and 8 were aggressive cancers. Of the 53 post-radiation prostate biopsies, 32 were benign tissues, 7 indolent/dying cancers, and 12 were aggressive (Table 2). The percentage of the biopsy cores that were positive for cancer ranged from 5 to 60% (14.0 ± 8.8%). No significant difference was observed between the average percentage of biopsy core positive for untreated and treated cancer samples or between the recurrent indolent and aggressive cancer samples.

Ki-67 labeling index was very low and not different between untreated predominately glandular and stromal benign samples (Table 2). For both untreated and post-radiation biopsy tissues, Ki-67 labeling index for aggressive cancer (11.0 ± 1.7% and 16.0 ± 3.3%, respectively) was significantly higher compared to benign (0.23 ± 0.14% and 0.10 ± 0.08%, respectively) and indolent cancer biopsies (1.40 ± 0.33% and 1.00 ±0.42%, respectively). Interestingly, benign tissues had a significant reduction and recurrent aggressive cancer had higher Ki-67 labeling after radiation therapy. Of particular importance to the current study, was a significant correlation between Ki-67 labeling index and [PC + GPC + free Cho] in both untreated (Spearman $\rho = 0.57$; $p < 0.001$) and irradiated (Spearman $\rho = 0.62$; $p < 0.001$) cancer biopsy specimens, and the majority of the (15 out of 17) cancers classified as aggressive by the Ki-67 staining had a primary Gleason 4 pattern (Gleason score ≥ 4+3)., and the other two had had ≥ 3+4 (Table 2).

Representative fully relaxed ^{1}H HR-MAS spectra of untreated predominately stromal (**A**), predominately glandular (**B**) benign prostate samples, and indolent (**C**), and aggressive cancer (**D**) samples are shown in Figure 2. Similar to previous HR-MAS studies of

surgically removed prostate tissues, predominately glandular biopsy benign tissues (Figure 2B) demonstrated high levels of citrate (doublet of doublets at 2.55 ppm) and polyamines (broad multiplet at 3.13 ppm), which were progressively reduced in both indolent and high-grade prostate cancer spectra (36,40–42). Predominantly benign stromal tissues also demonstrated a significant reduction ($p \leq 0.001$) in citrate and polyamines relative to benign glandular tissues (Figure 2, Table 3). In cancer there was also a clear increase in the free Cho (3.21 ppm), PC (3.23 ppm) and GPC (3.24 ppm) resonances in prostate cancer relative to benign glandular and stromal prostate tissues. Quantitatively, these observations proved true, with the concentration of citrate and polyamines being significantly lower and phospholipid metabolites significantly higher in prostate cancer relative to benign prostate tissues (Table 3). Moreover there was a significant increase in the concentration of phospholipid metabolites, [PC + GPC + free Cho], between benign and indolent cancer biopsies and between indolent and aggressive cancers (Figure 4A and Table 3). However, there was overlap of individual [PC + GPC + free Cho] values in indolent cancer with both benign and aggressive cancer biopsy tissues (Figure 4A). Other lower signal to noise prostate metabolites also demonstrated significant differences in their concentrations between untreated cancer and benign samples. These included significant increases in glutamate (multiplet at 2.35 ppm), alanine (doublet at 1.48 ppm) and lactate (doublet at 1.33 ppm) (Figure 4C) in untreated cancer relative to benign biopsies (Table 3).

Representative fully relaxed ^{1}H HR-MAS spectra of radiation-treated benign prostate samples (A), and indolent (B), and aggressive cancer (C) samples are shown in Figure 3. Effective radiation therapy induces glandular atrophy resulting in irradiated benign prostatic tissues being predominately stromal tissue (Figure 3A) similar to untreated benign stromal tissues (Figure 2A). Since citrate and polyamine production are associated with glandular prostate tissues not stroma (55), there was a loss of citrate and polyamines in irradiated benign tissues (Figure 3A). A number of post radiation benign and malignant tissues did retain some glandular architecture and had detectable levels of polyamines and citrate in the associated ^{1}H HR-MAS spectra. In both irradiated benign and malignant tissues, there was a significant reduction in [PC + GPC + free Cho], but the concentration of phospholipid metabolites in recurrent malignant tissues remained significantly higher than in irradiated benign tissues (Table 4). Similar to pre-treatment (Figure 4A), there was an increase in [PC + GPC + free Cho] between benign, indolent and aggressive cancer biopsies (Figure 4B and Table 4). Of particular importance to the current study, [PC + GPC + free Cho] was significantly higher in aggressive recurrent cancer than in benign tissues and indolent/dying tumors (Figure 4B and Table 4). [Lactate] was also significantly higher in post-radiation residual prostate cancer relative to benign tissue, but did not discriminate aggressive and indolent recurrent cancer (Figure 4D and Table 4). The amplitudes of glutamate and alanine were typically reduced to noise level of ^{1}H HR-MAS spectra after radiation therapy and therefore were not useful as biomarkers of cancer presence or aggressiveness.

Figure 5 demonstrates the upper diagonal CH_2-CH_2 region of the 2D TOCSY spectra from the representative untreated and irradiated aggressive cancer biopsies shown in Figures 2D and 3C. On visual inspection, GPC cross-peaks were higher than PC in untreated cancer *versus* post-radiation cancer biopsy tissues. Quantitatively, these observations proved true with [GPC] and [PC] being the most dominant phospholipid metabolites in untreated and treated aggressive cancers, respectively. Specifically, in untreated aggressive cancer tissues, [GPC] was 1.10 ± 0.46 mmolal, almost 2-fold higher than [PC] (0.60 ± 0.20 mmolal). On the contrary, in post-radiation aggressive cancer tissues, [PC] was 0.96 ± 0.21 mmolal, more than 7-fold higher than [GPC] (0.13 ± 0.06 mmolal). On average, the post radiation biopsies studied had a significantly ($p \leq 0.001$) higher Ki-67 labeling index and were of higher pathologic grade (Table 2).

Figure 6 is a ROC curve demonstrating the performance of using the total choline to creatine ratio, [PC + GPC + free Cho]/[Cr], to predict aggressive recurrent prostate cancer after radiation therapy. Creatine concentration did not significantly change between benign (1.30 ± 0.10 mmolal), indolent (1.31 ± 0.22 mmolal) and aggressive cancer (1.30 +− 0.22 mmolal) tissues after radiation therapy. Therefore the total choline-to-creatine ratio can be used in *in vivo* ^{1}H MRSI studies where concentrations are difficult to measure. The mean tCho/Cr concentration ratio significantly ($p = 0.02$) increased in indolent (0.50 ± 0.09) cancer *versus* benign tissues (0.38 ± 0.04) and in aggressive cancer (0.82 ± 0.17) *versus* indolent cancer ($p \leq 0.005$). Since the choline and creatine head-groups have 9 and 3 equivalent protons and similar T_1 and T_2 relaxation times (56), respectively, the *in vivo* tCho/Cr peak ratio will be approximately 3 times larger than the concentration ratio (1.1 ± 0.1, 1.5 ± 0.2 and 2.4 ± 0.4 for benign, indolent, and aggressive recurrent cancer, respectively). The area under the ROC curve for predicting aggressive cancer using [PC + GPC + free Cho]/[Cr] ratio was 0.95 (confidence interval = 0.88 to 1.00).

DISCUSSION

A growing number of prostate cancer patients receiving multiparametric ^{1}H MR exams are referred for suspected local cancer recurrence after radiation therapy. Recurrent cancer is typically suspected in these patients due to a detectable or rising PSA (3), however as demonstrated in this study, even patients with aggressive recurrent cancer often have much lower PSA concentrations than those with similar cancer burdens prior to therapy (3.40 ± 0.91 *versus* 19 ± 13 ng/mL for aggressive recurrent cancer and aggressive untreated cancer patients). This is most likely due to the reduction in contribution of serum PSA arising from benign prostate tissues effectively treated during radiation therapy, since a significant amount of serum PSA arises from benign prostate tissues.

The identification of recurrent prostate cancer after radiation by either a PSA nadir or pathology of subsequent prostate biopsies is further confounded by the relatively slow rate of radiation-induced cellular death (28), and radiation-induced pathologic changes (6–8), resulting in the inability to accurately predict clinical progressive recurrent cancer within the first two years after radiation therapy. However, prior published studies have associated high cellular staining of the nuclear antigen Ki-67 with high pathologic grade prostate cancer (31–33) and with subsequent local failure of radiation therapy of prostate cancer (8,34,35). Using greater than 5% Ki-67 staining of prostate cancer as a measure of recurrent aggressive cancer (8,34,35), this study demonstrated that the concentration of phospholipid metabolites, [PC + GPC + free Cho], was significantly higher in these recurrent tumors as compared to both benign tissues and/or indolent/dying tumors after radiation therapy. Moreover, the majority of cancers classified as aggressive by Ki-67 staining had a primary Gleason 4 cancer (Gleason score ≥ 4+3), a pathologic pattern considered to be clinically aggressive/progressive disease (57,58). The ability to discriminate recurrent aggressive cancer following radiation therapy has clinical significance, as the detection of residual cancer at an earlier time after treatment could allow earlier intervention with additional salvage therapy.

The 2D TOCSY HR-MAS data also demonstrated that glycerophosphocholine was the dominant choline-containing phospholipid metabolite in aggressive untreated human prostate cancer tissue (PC/GPC = 0.6), which is in agreement with prior studies of surgical human prostate specimens (36,40). Whereas phosphocholine was found to be the dominant phospholipid metabolite with GPC being dramatically reduced (PC/GPC = 7.6) in recurrent aggressive prostate cancer after radiation therapy. In previous studies of culture-immortalized (37) and primary human prostate cancer cells (39), [PC] was also the dominant phospholipid. PC and GPC serve as a precursor and a degradation product of phospholipid metabolism, respectively. Enhanced [PC]/[GPC] ratio has been suggested to indicate tumor

progression from lower to higher malignancy grades in breast cancer cell lines and brain tumors (38,59–63). PC has also been proposed to be mitogenic by acting as a mediator of growth factor-induced cell proliferation (38,61,63–65). The [PC]/[GPC] ratio difference observed in this study between untreated and post-radiation residual prostate cancer, especially in high-proliferative cancer specimens, might be a result of the survival of a more aggressive cell phenotype with higher radio-resistance following radiation therapy. Several clinical studies have shown that conventional-dose radiation therapy does not eradicate prostate cancer in a significant proportion of cases, leading to eventual clinical recurrence (66,67).

The concentration of lactate was also found to be significantly higher in post-radiation residual prostate cancer relative to benign tissue, but [lactate] did not reach statistical significance in discriminating aggressive and indolent recurrent cancer. The significant increase in lactate concentrations found in both untreated and post-radiation residual prostate cancer is in agreement with previous ^{1}H HR-MAS study of prostate tissues (48) and other human cancers (68–71). *In vivo* prostate lactate levels have not been typically monitored by ^{1}H MRSI studies of patients due to complications with overlapping lipid. However, with improved volume selection, outer voxel suppression techniques, and higher-field (3T) scanners, it is becoming feasible to use spectral-spatial RF editing sequences to detect lactate (72). Additionally, new hyperpolarized ^{13}C MR techniques could potentially take advantage of elevated lactate in proliferating residual cancer after radiation therapy. Elevated hyperpolarized [1-^{13}C] lactate levels have been shown to correlate with prostate cancer grade (47), and with failed androgen deprivation therapy in the transgenic adenocarcinoma of mouse prostate (TRAMP) model (73). Hyperpolarized [1-^{13}C] lactate levels have also been shown to be a sensitive index of radiation-induced biochemical changes (74,75). Therefore, the changes in lactate observed in the present study could be used to improve clinical diagnosis and monitoring of prostate cancer progression after radiation therapy using hyperpolarized ^{13}C MR techniques.

Other prostate metabolites, including citrate, polyamines, alanine, and glutamate, which demonstrated significant differences in their concentrations between untreated cancer and benign biopsy tissues in this study and in a number of prior *in vivo* ^{1}H MRSI (16,44–46,76) and *ex vivo* ^{1}H HR-MAS spectroscopy studies (41,42,48,77), were typically reduced to noise level in ^{1}H HR-MAS spectra of post radiation biopsies. Since radiation therapy induces glandular atrophy, effectively irradiated benign prostatic tissues were observed to be pathologically similar to untreated benign stromal tissues, with an associated loss of the prostatic secretory metabolites polyamines and citrate in the ^{1}H HR-MAS spectra. The time-dependent loss of citrate and polyamines in both benign and malignant tissues after radiation therapy has been observed in several serial ^{1}H MRSI studies of prostate cancer patients (17,18). Additionally, prostate tissues receiving insufficient doses of radiation in these *in vivo* studies often had ^{1}H MRSI spectra containing observable citrate and polyamine metabolite resonances and the associated prostate tissue presumably retained some glandular architecture (17,18) similar to the glandular pathology that was observed in a number of post-radiation biopsies that also demonstrated ^{1}H HR-MAS spectra detectable citrate and polyamine concentrations. There was also an approximate 50% reduction in the concentration of all prostate metabolites reliably detected in both pre-treated and irradiated biopsy tissues, but the concentration of the choline-containing phospholipid metabolites remained in the *in vivo* ^{1}H MRSI detectable millimolar concentration range and were approximately 3 fold higher than irradiated benign tissues and approximately 2 fold higher than recurrent indolent cancer biopsies. Indeed, successful radiation treatment has been characterized by *in vivo* ^{1}H MRSI as a lack of metabolic activity or “metabolic atrophy” (17,18). Whereas, recurrent prostate cancer can be detected by *in vivo* ^{1}H MRSI based on an elevated *in vivo* total choline resonance (11,19).

Since absolute concentrations of individual choline-containing phospholipid metabolites are very difficult to measure using *in vivo* ^{1}H MRSI, the total choline to creatine ratio has been used to identify recurrent prostate cancer after radiation (11,19). In this study, the concentration of creatine did not significantly change between benign, indolent and aggressive cancer biopsy tissues after radiation therapy, indicating that the changes observed in the total choline to creatine ratio after radiation predominately reflect changes in the concentration of choline-containing phospholipid metabolites. There was significant changes in the mean tCho/Cr ratio between benign indolent and aggressive cancer tissues after radiation therapy, and the area under the ROC curve analysis of tCho/Cr demonstrated an accuracy of 95% (confidence interval = 0.88 to 1.00) for predicting aggressive recurrent disease. These findings are consistent with prior MRI/^{1}H MRSI studies of prostate cancer patients after radiation therapy demonstrating that tCho/Cr provided the most accurate predictor of the presence of recurrent cancer after radiation therapy (11,19). The mean tCho/Cr ratio threshold for the detection of any (indolent or aggressive) recurrent cancer ($\geq 1.5 \pm 0.2$) after radiation in this study was not different from the ratio that was determined from a ROC analysis of prior *in vivo* data (tCho/Cr threshold ratio of ≥ 1.5). The tCho/Cr ratio was significantly higher for identifying aggressive cancer ($tCho/Cr = 2.4 \pm 0.4$) suggesting that a higher threshold tCho/Cr ratio could improve the selection and therapeutic planning of patients that would benefit most from salvage focal therapy after failed radiation therapy.

This study has several limitations. Although biopsy tissues provided a more accurate snapshot of *in vivo* metabolism, there were a number of contaminants compared to surgical samples. These contaminants arose from periprostatic lipid contamination and the topical anesthetic (Hurricaine®; Beulich) that was applied prior to the TRUS procedure. This resulted in 5 (~6%) prostate biopsy samples being unusable for determining lactate concentrations. The lack of significance of lactate concentration to predict recurrent aggressive cancer could be due to this smaller sample size since there was trend towards significance. Additionally, only two additional research biopsies could be obtained per patient and the sample sizes were much smaller than what can be obtained from surgical specimens. Nevertheless, the use of snap-frozen biopsy tissues was critical for this study in order to minimize the impact of anaerobic glycolysis, which occurs in surgical specimens. We attempted to overcome the subjectivity of determining cancer percentage, Ki-67 labeling index and cancer grade for biopsies by averaging duplicate readings of two prostate pathologists with extensive experience, but a more quantitative pathologic approach would be important in future studies (78). Another limitation of this study was the variability of the cancer percentage within the biopsy tissues used. This is an unfortunate consequence of the fact that many TRUS – guided biopsy tissues obtained have very small amounts of prostate cancer. We found that correcting the samples for percentage cancer was problematic for specimens containing small amounts of prostate cancer. However, to minimize the impact of the % cancer on the statistical comparison of tissue types before and after radiation therapy, we made sure there was no significant difference was observed between the average percentage of biopsy core positive for untreated and treated cancer samples or between the recurrent indolent and aggressive cancer samples. Most likely, the differences between benign, indolent and aggressive cancer would be even more significant if tissues could be obtained with higher percentages of cancer. Future studies could use direct MR-guided biopsies, recently approved by the Food and Drug Administration (79) to provide improved the collection of higher percentages of cancer from the dominant lesion in the prostate.

CONCLUSIONS

This study demonstrated that the concentrations of phospholipid metabolites (PC, GPC and free Cho), and lactate were significantly elevated in recurrent cancer as compared to surrounding benign tissues. There was also a significant increase in phosphocholine

concentration and reduction in glycerophosphocholine concentration between untreated and irradiated prostate cancer biopsies that were associated with significantly higher Ki-67 staining indices and pathologic grade. Other prostate metabolites, including citrate, polyamines, alanine, and glutamate which demonstrated significant differences in their concentrations between untreated cancer and benign biopsy tissues were typically reduced to the noise level of ^{1}H HR-MAS spectra for post radiation biopsies. The concentration of the choline-containing phospholipid metabolites and the associated total choline to creatine ratio in recurrent aggressive cancer was significantly higher than irradiated benign tissues (≈3 fold) and recurrent indolent cancer biopsies (≈ 2 fold). These results support the role of *in vivo* ^{1}H MRSI to discriminate between aggressive/progressive and indolent dying prostate cancer following radiation therapy based on the magnitude of elevation of the *in vivo* total choline to creatine ratio. This hypothesis will need to be tested through future *in vivo* multiparametric MR studies of patients with rising PSA after failed radiation therapy.

Acknowledgments

We would like to thank Dr. Jeff Simko for reviewing the pathology slides. We want to thank, Mark G. Swanson, Rahwa Iman and Thomas Butler for acquiring some of the HR-MAS data. We also want to thank Maria Grinde for some of the initial HR-MAS data processing.

This research was funded by the following grants: National Institute of Health (NIH): NIH R01- CA137207, R01-CA059897, R01-CA111291.

Abbreviations

HR-MAS	High resolution magic angle spinning
MR	Magnetic resonance
1D	One dimensional
2D	Two dimensional
TR	Repetition time
TRUS	Transrectal ultrasound
PSA	Prostate specific antigen
PIN	Prostatic intraepithelial neoplasia
BPH	Benign prostatic hyperplasia
OCT	Optimal cutting temperature
TOCSY	Total correlation spectroscopy
TSP	3-(trimethylsilyl)propionic-2,2,3,3-d4 acid
H&E	Hematoxylin and eosin
Cho	Choline
PC	Phosphocholine
GPC	Glycerophosphocholine
tCho	Total choline
Cr	Creatine
PA	Polyamines
MyoI	Myo-inositol

Glu	Glutamate
Ala	Alanine
Lac	Lactate
PE	Phosphoethanolamine
GPE	Glycerophosphoethanolamine
Eth	Ethanolamine
ERETIC	Electronic reference to access to *in vivo* concentrations
HR-QUEST	High resolution quantum estimation
jMRUI	Java-based graphical user interface for the magnetic resonance user interface
CRLB	Cramér – Rao Lower Bounds
MRSI	Magnetic resonance spectroscopy imaging
ROC	Receiver operating characteristic
AUC	Area under the receiver operating characteristic curve
ADC	Apparent diffusion coefficient
DCE	Dynamic contrast enhancement
DWI	Diffusion weighted imaging
TRAMP	Transgenic adenocarcinoma of the mouse prostate

References

1. Siegel R, Naishadham D, Jemal A. Cancer statistics, 2012. CA Cancer J Clin. 2012; 62(1):10–29. [PubMed: 22237781]
2. Cooperberg MR, Broering JM, Carroll PR. Time trends and local variation in primary treatment of localized prostate cancer. J Clin Oncol. 2010; 28(7):1117–1123. [PubMed: 20124165]
3. Kuban DA, Thames HD, Levy LB, Horwitz EM, Kupelian PA, Martinez AA, Michalski JM, Pisansky TM, Sandler HM, Shipley WU, Zelefsky MJ, Zietman AL. Long-term multi-institutional analysis of stage T_1-T_2 prostate cancer treated with radiotherapy in the PSA era. Int J Radiat Oncol Biol Phys. 2003; 57(4):915–928. [PubMed: 14575822]
4. Vo T, Rifkin MD, Peters TL. Should ultrasound criteria of the prostate be redefined to better evaluate when and where to biopsy. Ultrasound Q. 2001; 17(3):171–176. [PubMed: 12973073]
5. Rabbani F, Stroumbakis N, Kava BR, Cookson MS, Fair WR. Incidence and clinical significance of false-negative sextant prostate biopsies. J Urol. 1998; 159(4):1247–1250. [PubMed: 9507846]
6. Cox JD, Kline RW. Do prostatic biopsies 12 months or more after external irradiation for adenocarcinoma, Stage III, predict long-term survival? Int J Radiat Oncol Biol Phys. 1983; 9(3): 299–303. [PubMed: 6404866]
7. Kuban DA, el-Mahdi AM, Schellhammer P. The significance of post-irradiation prostate biopsy with long-term follow-up. Int J Radiat Oncol Biol Phys. 1992; 24(3):409–414. [PubMed: 1399724]
8. Crook J, Malone S, Perry G, Bahadur Y, Robertson S, Abdolell M. Postradiotherapy prostate biopsies: what do they really mean? Results for 498 patients. Int J Radiat Oncol Biol Phys. 2000; 48(2):355–367. [PubMed: 10974448]
9. Hanlon AL, Diratzouian H, Hanks GE. Posttreatment prostate-specific antigen nadir highly predictive of distant failure and death from prostate cancer. Int J Radiat Oncol Biol Phys. 2002; 53(2):297–303. [PubMed: 12023133]

10. Kestin LL, Vicini FA, Ziaja EL, Stromberg JS, Frazier RC, Martinez AA. Defining biochemical cure for prostate carcinoma patients treated with external beam radiation therapy. Cancer. 1999; 86(8):1557–1566. [PubMed: 10526285]
11. Pickett B, Kurhanewicz J, Coakley F, Shinohara K, Fein B, Roach M 3rd. Use of MRI and spectroscopy in evaluation of external beam radiotherapy for prostate cancer. International journal of radiation oncology, biology, physics. 2004; 60(4):1047–1055.
12. Pucar D, Shukla-Dave A, Hricak H, Moskowitz CS, Kuroiwa K, Olgac S, Ebora LE, Scardino PT, Koutcher JA, Zakian KL. Prostate cancer: correlation of MR imaging and MR spectroscopy with pathologic findings after radiation therapy-initial experience. Radiology. 2005; 236(2):545–553. [PubMed: 15972335]
13. Sala E, Eberhardt SC, Akin O, Moskowitz CS, Onyebuchi CN, Kuroiwa K, Ishill N, Zelefsky MJ, Eastham JA, Hricak H. Endorectal MR imaging before salvage prostatectomy: tumor localization and staging. Radiology. 2006; 238(1):176–183. [PubMed: 16373766]
14. Westphalen AC, Kurhanewicz J, Cunha RM, Hsu IC, Kornak J, Zhao S, Coakley FV. T_2-Weighted endorectal magnetic resonance imaging of prostate cancer after external beam radiation therapy. Int Braz J Urol. 2009; 35(2):171–180. discussion 181–172. [PubMed: 19409121]
15. Kurhanewicz J, Vigneron DB, Hricak H, Narayan P, Carroll P, Nelson SJ. Three-dimensional ^{1}H MR spectroscopic imaging of the in situ human prostate with high (0.24–0. 7 cm^3) spatial resolution. Radiology. 1996; 198(3):795–805. [PubMed: 8628874]
16. Kurhanewicz J, Vigneron DB, Males RG, Swanson MG, Yu KK, Hricak H. The prostate: MR imaging and spectroscopy. Present and future Radiol Clin North Am. 2000; 38(1):115–138. viii–ix.
17. Pickett B, Ten Haken RK, Kurhanewicz J, Qayyum A, Shinohara K, Fein B, Roach M 3rd. Time to metabolic atrophy after permanent prostate seed implantation based on magnetic resonance spectroscopic imaging. Int J Radiat Oncol Biol Phys. 2004; 59(3):665–673. [PubMed: 15183469]
18. Roach M 3rd, Kurhanewicz J, Carroll P. Spectroscopy in prostate cancer: hope or hype? Oncology (Williston Park). 2001; 15(11):1399–1410. discussion 1415–1396, 1418. [PubMed: 11758871]
19. Westphalen AC, Coakley FV, Roach M 3rd, McCulloch CE, Kurhanewicz J. Locally recurrent prostate cancer after external beam radiation therapy: diagnostic performance of 1. 5-T endorectal MR imaging and MR spectroscopic imaging for detection. Radiology. 2010; 256(2):485–492. [PubMed: 20551184]
20. Kim CK, Park BK, Lee HM. Prediction of locally recurrent prostate cancer after radiation therapy: incremental value of 3T diffusion-weighted MRI. J Magn Reson Imaging. 2009; 29(2):391–397. [PubMed: 19161194]
21. Westphalen AC, Reed GD, Vinh PP, Sotto C, Vigneron DB, Kurhanewicz J. Multiparametric 3T endorectal mri after external beam radiation therapy for prostate cancer. Journal of magnetic resonance imaging: JMRI. 2012; 36(2):430–437. [PubMed: 22535708]
22. Haider MA, Chung P, Sweet J, Toi A, Jhaveri K, Menard C, Warde P, Trachtenberg J, Lockwood G, Milosevic M. Dynamic contrast-enhanced magnetic resonance imaging for localization of recurrent prostate cancer after external beam radiotherapy. Int J Radiat Oncol Biol Phys. 2008; 70(2):425–430. [PubMed: 17881141]
23. Bong GW, Keane TE. Salvage options for biochemical recurrence after primary therapy for prostate cancer. Can J Urol. 2007; 14 (Suppl 1):2–9. [PubMed: 18163938]
24. Hsu CC, Hsu H, Pickett B, Crehange G, Hsu IC, Dea R, Weinberg V, Gottschalk AR, Kurhanewicz J, Shinohara K, Roach M 3rd. Feasibility of MR Imaging/MR Spectroscopy-Planned Focal Partial Salvage Permanent Prostate Implant (PPI) for Localized Recurrence After Initial PPI for Prostate Cancer. International journal of radiation oncology, biology, physics. 2012
25. Jabbari S, Hsu IC, Kawakami J, Weinberg VK, Speight JL, Gottschalk AR, Roach M 3rd, Shinohara K. High-dose-rate brachytherapy for localized prostate adenocarcinoma post abdominoperineal resection of the rectum and pelvic irradiation: Technique and experience. Brachytherapy. 2009; 8(4):339–344. [PubMed: 19428310]
26. Lee B, Shinohara K, Weinberg V, Gottschalk AR, Pouliot J, Roach M 3rd, Hsu IC. Feasibility of high-dose-rate brachytherapy salvage for local prostate cancer recurrence after radiotherapy: the

University of California-San Francisco experience. Int J Radiat Oncol Biol Phys. 2007; 67(4): 1106–1112. [PubMed: 17197119]

27. Moman MR, van den Berg CA, Boeken Kruger AE, Battermann JJ, Moerland MA, van der Heide UA, van Vulpen M. Focal salvage guided by T_2-weighted and dynamic contrast-enhanced magnetic resonance imaging for prostate cancer recurrences. Int J Radiat Oncol Biol Phys. 76(3): 741–746. [PubMed: 19804948]
28. Mostofi FK, Sesterhenn IA, Davis CJ Jr. A pathologist's view of prostatic carcinoma. Cancer. 1993; 71(3 Suppl):906–932. [PubMed: 7679044]
29. Pickett B, Kurhanewicz J, Pouliot J, Weinberg V, Shinohara K, Coakley F, Roach M 3rd. Three-dimensional conformal external beam radiotherapy compared with permanent prostate implantation in low-risk prostate cancer based on endorectal magnetic resonance spectroscopy imaging and prostate-specific antigen level. International journal of radiation oncology, biology, physics. 2006; 65(1):65–72.
30. Foltz WD, Wu A, Chung P, Catton C, Bayley A, Milosevic M, Bristow R, Warde P, Simeonov A, Jaffray DA, Haider MA, Menard C. Changes in apparent diffusion coefficient and T_2 relaxation during radiotherapy for prostate cancer. Journal of magnetic resonance imaging: JMRI. 2012
31. Feneley MR, Young MP, Chinyama C, Kirby RS, Parkinson MC. Ki-67 expression in early prostate cancer and associated pathological lesions. Journal of Clinical Pathology. 1996; 49(9): 741–748. [PubMed: 9038759]
32. Pollack A, DeSilvio M, Khor L, Li R, Al-Saleem T, Hammond M, Venkatesan V, Byhardt R, Hanks GE, Roach M, Shipley WU, Sandler HM. Ki-67 staining is a strong predictor of patient outcome for prostate cancer patients treated with androgen deprivation plus radiotherapy: an analysis of RTOG 92-02. Int J Radiat Oncol Biol Phys. 2003; 57(2 Suppl):S200–201.
33. Pollack A, DeSilvio M, Khor LY, Li R, Al-Saleem TI, Hammond ME, Venkatesan V, Lawton CA, Roach M 3rd, Shipley WU, Hanks GE, Sandler HM. Ki-67 staining is a strong predictor of distant metastasis and mortality for men with prostate cancer treated with radiotherapy plus androgen deprivation: Radiation Therapy Oncology Group Trial 92-02. Journal of clinical oncology: official journal of the American Society of Clinical Oncology. 2004; 22(11):2133–2140. [PubMed: 15169799]
34. Parker AS, Heckman MG, Wu KJ, Crook JE, Hilton TW, Pisansky TM, Bernard JR, Schild SE, Khor LY, Hammond EH, Pollack A, Buskirk SJ. Evaluation of Ki-67 staining levels as an independent biomarker of biochemical recurrence after salvage radiation therapy for prostate cancer. Int J Radiat Oncol Biol Phys. 2009; 75(5):1364–1370. [PubMed: 19464826]
35. Khor LY, Bae K, Paulus R, Al-Saleem T, Hammond ME, Grignon DJ, Che M, Venkatesan V, Byhardt RW, Rotman M, Hanks GE, Sandler HM, Pollack A. MDM2 and Ki-67 predict for distant metastasis and mortality in men treated with radiotherapy and androgen deprivation for prostate cancer: RTOG 92-02. J Clin Oncol. 2009; 27(19):3177–3184. [PubMed: 19470936]
36. Keshari KR, Tsachres H, Iman R, Delos Santos L, Tabatabai ZL, Shinohara K, Vigneron DB, Kurhanewicz J. Correlation of phospholipid metabolites with prostate cancer pathologic grade, proliferative status and surgical stage - impact of tissue environment. NMR Biomed. 2011; 24(6): 691–699. [PubMed: 21793074]
37. Ackerstaff E, Pflug BR, Nelson JB, Bhujwalla ZM. Detection of increased choline compounds with proton nuclear magnetic resonance spectroscopy subsequent to malignant transformation of human prostatic epithelial cells. Cancer Res. 2001; 61(9):3599–3603. [PubMed: 11325827]
38. Glunde K, Ackerstaff E, Mori N, Jacobs MA, Bhujwalla ZM. Choline phospholipid metabolism in cancer: consequences for molecular pharmaceutical interventions. Mol Pharm. 2006; 3(5):496–506. [PubMed: 17009848]
39. Levin YS, Albers MJ, Butler TN, Spielman D, Peehl DM, Kurhanewicz J. Methods for metabolic evaluation of prostate cancer cells using proton and ^{13}C HR-MAS spectroscopy and [3-^{13}C] pyruvate as a metabolic substrate. Magn Reson Med. 2009; 62(5):1091–1098. [PubMed: 19780158]
40. Swanson MG, Keshari KR, Tabatabai ZL, Simko JP, Shinohara K, Carroll PR, Zektzer AS, Kurhanewicz J. Quantification of choline- and ethanolamine-containing metabolites in human prostate tissues using ^{1}H HR-MAS total correlation spectroscopy. Magn Reson Med. 2008; 60(1): 33–40. [PubMed: 18581409]

41. Swanson MG, Vigneron DB, Tabatabai ZL, Males RG, Schmitt L, Carroll PR, James JK, Hurd RE, Kurhanewicz J. Proton HR-MAS spectroscopy and quantitative pathologic analysis of MRI/3D-MRSI-targeted postsurgical prostate tissues. Magn Reson Med. 2003; 50(5):944–954. [PubMed: 14587005]
42. Swanson MG, Zektzer AS, Tabatabai ZL, Simko J, Jarso S, Keshari KR, Schmitt L, Carroll PR, Shinohara K, Vigneron DB, Kurhanewicz J. Quantitative analysis of prostate metabolites using ^{1}H HR-MAS spectroscopy. Magn Reson Med. 2006; 55(6):1257–1264. [PubMed: 16685733]
43. Kurhanewicz J, Swanson MG, Nelson SJ, Vigneron DB. Combined magnetic resonance imaging and spectroscopic imaging approach to molecular imaging of prostate cancer. J Magn Reson Imaging. 2002; 16(4):451–463. [PubMed: 12353259]
44. Casciani E, Polettini E, Bertini L, Emiliozzi P, Amini M, Pansadoro V, Gualdi GF. Prostate cancer: evaluation with endorectal MR imaging and three-dimensional proton MR spectroscopic imaging. Radiol Med. 2004; 108(5–6):530–541. [PubMed: 15722999]
45. Kumar R, Kumar M, Jagannathan NR, Gupta NP, Hemal AK. Proton magnetic resonance spectroscopy with a body coil in the diagnosis of carcinoma prostate. Urological Research. 2004; 32(1):36–40. [PubMed: 14534764]
46. Zakian KL, Sircar K, Hricak H, Chen HN, Shukla-Dave A, Eberhardt S, Muruganandham M, Ebora L, Kattan MW, Reuter VE, Scardino PT, Koutcher JA. Correlation of proton MR spectroscopic imaging with gleason score based on step-section pathologic analysis after radical prostatectomy. Radiology. 2005; 234(3):804–814. [PubMed: 15734935]
47. Albers MJ, Bok R, Chen AP, Cunningham CH, Zierhut ML, Zhang VY, Kohler SJ, Tropp J, Hurd RE, Yen YF, Nelson SJ, Vigneron DB, Kurhanewicz J. Hyperpolarized ^{13}C lactate, pyruvate, and alanine: noninvasive biomarkers for prostate cancer detection and grading. Cancer Res. 2008; 68(20):8607–8615. [PubMed: 18922937]
48. Tessem MB, Swanson MG, Keshari KR, Albers MJ, Joun D, Tabatabai ZL, Simko JP, Shinohara K, Nelson SJ, Vigneron DB, Gribbestad IS, Kurhanewicz J. Evaluation of lactate and alanine as metabolic biomarkers of prostate cancer using ^{1}H HR-MAS spectroscopy of biopsy tissues. Magn Reson Med. 2008; 60(3):510–516. [PubMed: 18727052]
49. Verma S, Rajesh A, Futterer JJ, Turkbey B, Scheenen TW, Pang Y, Choyke PL, Kurhanewicz J. Prostate MRI and 3D MR spectroscopy: how we do it. AJR American journal of roentgenology. 2010; 194(6):1414–1426. [PubMed: 20489079]
50. Albers MJ, Butler TN, Rahwa I, Bao N, Keshari KR, Swanson MG, Kurhanewicz J. Evaluation of the ERETIC method as an improved quantitative reference for ^{1}H HR-MAS spectroscopy of prostate tissue. Magn Reson Med. 2009; 61(3):525–532. [PubMed: 19235261]
51. Naressi A, Couturier C, Devos JM, Janssen M, Mangeat C, de Beer R, Graveron-Demilly D. Java-based graphical user interface for the MRUI quantitation package. MAGMA. 2001; 12(2–3):141–152. [PubMed: 11390270]
52. Ratiney H, Albers MJ, Rabeson H, Kurhanewicz J. Semi-parametric time-domain quantification of HR-MAS data from prostate tissue. NMR Biomed. 2010; 23(10):1146–1157. [PubMed: 20842756]
53. Swanson, MGNS.; Kurhanewicz, J. Magnetic Resonance Spectroscopy and Spectroscopic Imaging of the Prostate, Breast, and Liver. In: WG, editor. Modern Magnetic Resonance. Vol. 1. Springer; The Netherlands: 2006. p. 1-13.
54. Diggle, P.; Liang, K-Y.; Zeger, SL. Analysis of longitudinal data. Vol. xi. Oxford University Press; 1994. p. 253
55. Costello LC, Franklin RB. Concepts of citrate production and secretion by prostate: 2. Hormonal relationships in normal and neoplastic prostate. Prostate. 1991; 19(3):181–205. [PubMed: 1946039]
56. Heerschap A, Jager GJ, van der Graaf M, Barentsz JO, Ruijs SH. Proton MR spectroscopy of the normal human prostate with an endorectal coil and a double spin-echo pulse sequence. Magnetic resonance in medicine: official journal of the Society of Magnetic Resonance in Medicine/Society of Magnetic Resonance in Medicine. 1997; 37(2):204–213. [PubMed: 9001144]

57. Egevad L, Granfors T, Karlberg L, Bergh A, Stattin P. Percent Gleason grade 4/5 as prognostic factor in prostate cancer diagnosed at transurethral resection. J Urol. 2002; 168(2):509–513. [PubMed: 12131299]
58. Wills ML, Sauvageot J, Partin AW, Gurganus R, Epstein JI. Ability of sextant biopsies to predict radical prostatectomy stage. Urology. 1998; 51(5):759–764. [PubMed: 9610589]
59. Bhujwalla ZM, Aboagye EO, Gillies RJ, Chacko VP, Mendola CE, Backer JM. Nm23-transfected MDA-MB-435 human breast carcinoma cells form tumors with altered phospholipid metabolism and pH: a ^{31}P nuclear magnetic resonance study *in vivo* and *in vitro*. Magn Reson Med. 1999; 41(5):897–903. [PubMed: 10332871]
60. Usenius JP, Vainio P, Hernesniemi J, Kauppinen RA. Choline-containing compounds in human astrocytomas studied by ^{1}H NMR spectroscopy *in vivo* and *in vitro*. J Neurochem. 1994; 63(4): 1538–1543. [PubMed: 7931308]
61. Podo F. Tumour phospholipid metabolism. NMR Biomed. 1999; 12(7):413–439. [PubMed: 10654290]
62. Aboagye EO, Bhujwalla ZM. Malignant transformation alters membrane choline phospholipid metabolism of human mammary epithelial cells. Cancer Res. 1999; 59(1):80–84. [PubMed: 9892190]
63. Podo F, Canevari S, Canese R, Pisanu ME, Ricci A, Iorio E. MR evaluation of response to targeted treatment in cancer cells. NMR Biomed. 2011; 24(6):648–672. [PubMed: 21387442]
64. Cuadrado A, Carnero A, Dolfi F, Jimenez B, Lacal JC. Phosphorylcholine: a novel second messenger essential for mitogenic activity of growth factors. Oncogene. 1993; 8(11):2959–2968. [PubMed: 8414498]
65. Negendank W. Studies of Human Tumors by Mrs - a Review. Nmr in Biomedicine. 1992; 5(5): 303–324. [PubMed: 1333263]
66. Kupelian PA, Potters L, Khuntia D, Ciezki JP, Reddy CA, Reuther AM, Carlson TP, Klein EA. Radical prostatectomy, external beam radiotherapy <72 Gy, external beam radiotherapy > or =72 Gy, permanent seed implantation, or combined seeds/external beam radiotherapy for stage T_1-T_2 prostate cancer. Int J Radiat Oncol Biol Phys. 2004; 58(1):25–33. [PubMed: 14697417]
67. Zietman AL, Chung CS, Coen JJ, Shipley WU. 10-year outcome for men with localized prostate cancer treated with external radiation therapy: results of a cohort study. J Urol. 2004; 171(1):210–214. [PubMed: 14665878]
68. Brizel DM, Schroeder T, Scher RL, Walenta S, Clough RW, Dewhirst MW, Mueller-Klieser W. Elevated tumor lactate concentrations predict for an increased risk of metastases in head-and-neck cancer. Int J Radiat Oncol Biol Phys. 2001; 51(2):349–353. [PubMed: 11567808]
69. Schwickert G, Walenta S, Sundfor K, Rofstad EK, Mueller-Klieser W. Correlation of high lactate levels in human cervical cancer with incidence of metastasis. Cancer Res. 1995; 55(21):4757–4759. [PubMed: 7585499]
70. Walenta S, Chau TV, Schroeder T, Lehr HA, Kunz-Schughart LA, Fuerst A, Mueller-Klieser W. Metabolic classification of human rectal adenocarcinomas: a novel guideline for clinical oncologists? J Cancer Res Clin Oncol. 2003; 129(6):321–326. [PubMed: 12827509]
71. Walenta S, Schroeder T, Mueller-Klieser W. Lactate in solid malignant tumors: potential basis of a metabolic classification in clinical oncology. Curr Med Chem. 2004; 11(16):2195–2204. [PubMed: 15279558]
72. Cunningham CH, Vigneron DB, Chen AP, Xu D, Hurd RE, Sailasuta N, Pauly JM. Design of symmetric-sweep spectral-spatial RF pulses for spectral editing. Magn Reson Med. 2004; 52(1): 147–153. [PubMed: 15236378]
73. Chen, AP.; Bok, B.; Zhang, VY.; Xu, D.; Veeraraghavan, S.; Hurd, RE.; Nelson, SJ.; Kurhanewicz, J.; Vigneron, DB. Serial hyperpolarized ^{13}C 3D-MRSI following therapy in a mouse model of prostate cancer. 16th Scientific Meeting and Exhibition of ISMRM; Toronto, Ontario. 3–9 May, 2008; program# 888
74. Day SE, Kettunen MI, Cherukuri MK, Mitchell JB, Lizak MJ, Morris HD, Matsumoto S, Koretsky AP, Brindle KM. Detecting response of rat C6 glioma tumors to radiotherapy using hyperpolarized [1- ^{13}C]pyruvate and ^{13}C magnetic resonance spectroscopic imaging. Magn Reson Med. 2011; 65(2):557–563. [PubMed: 21264939]

75. Zhang, VY.; Bok, R.; Sukumar, S.; Cunha, A.; Hsu, IC.; Pouliot, J.; Vigneron, D.; Kurhanewicz, J. Detecting Early Tumor Response of Prostate Cancer to Radiation Therapy Using Multi-Parametric 14T ^{1}H and Hyperpolarized ^{13}C MR Imaging. 20th Scientific Meeting and Exhibition of ISMRM; Melbourne, Australia. 5–11 May, 2012; program# 4319

76. Garcia-Martin ML, Adrados M, Ortega MP, Fernandez Gonzalez I, Lopez-Larrubia P, Viano J, Garcia-Segura JM. Quantitative ^{1}H MR spectroscopic imaging of the prostate gland using LCModel and a dedicated basis-set: correlation with histologic findings. Magn Reson Med. 2011; 65(2):329–339. [PubMed: 20939087]

77. Cheng LL, Burns MA, Taylor JL, He W, Halpern EF, McDougal WS, Wu CL. Metabolic characterization of human prostate cancer with tissue magnetic resonance spectroscopy. Cancer Res. 2005; 65(8):3030–3034. [PubMed: 15833828]

78. Burns MA, He W, Wu CL, Cheng LL. Quantitative pathology in tissue MR spectroscopy based human prostate metabolomics. Technol Cancer Res Treat. 2004; 3(6):591–598. [PubMed: 15560717]

79. Hambrock T, Somford DM, Hoeks C, Bouwense SA, Huisman H, Yakar D, van Oort IM, Witjes JA, Futterer JJ, Barentsz JO. Magnetic resonance imaging guided prostate biopsy in men with repeat negative biopsies and increased prostate specific antigen. J Urol. 2010; 183(2):520–527. [PubMed: 20006859]

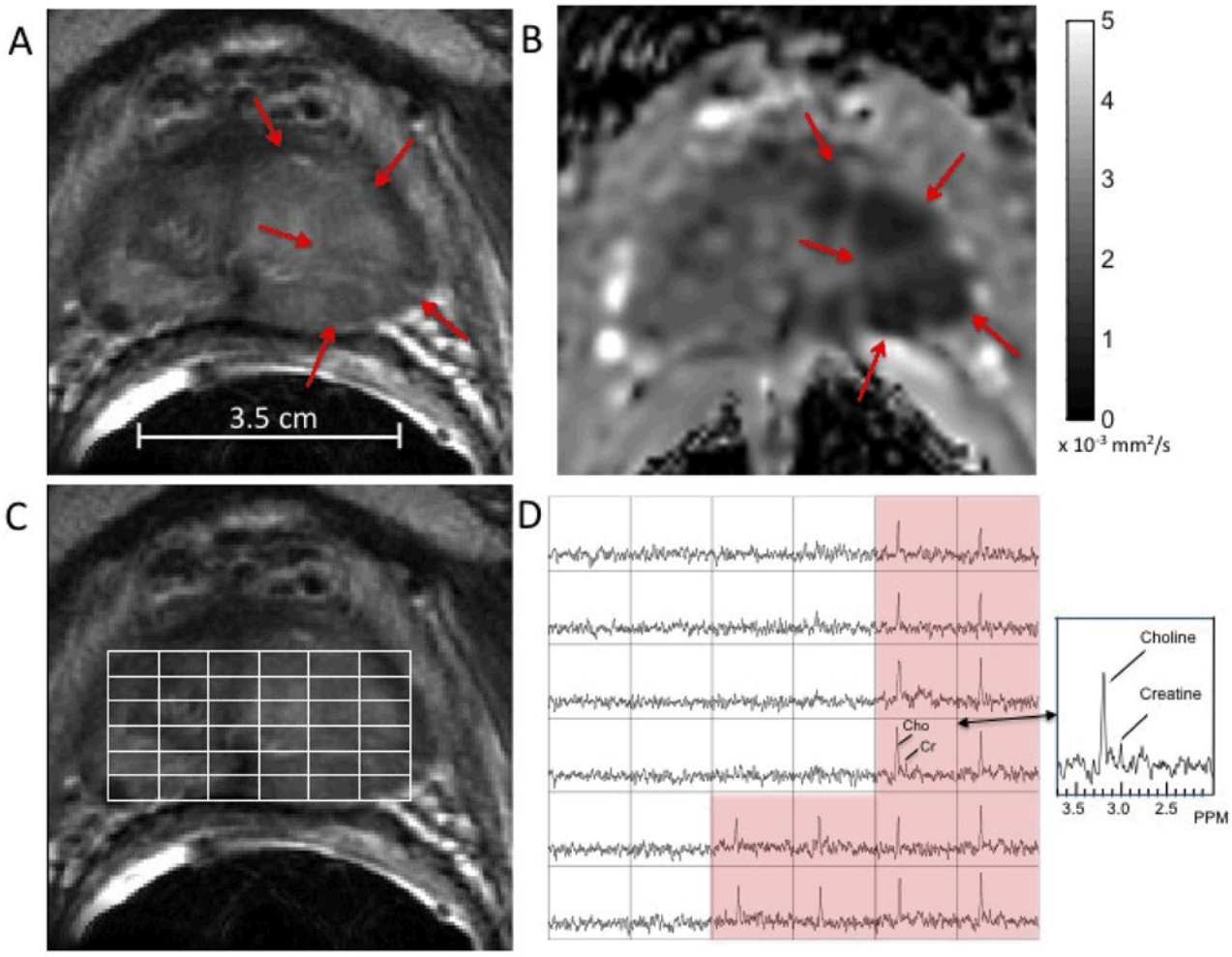

Figure 1.

(A) Representative T_2 - weighted axial image of a 63 year old patient with a PSA of 2.4 ng/ml, 2.5 years after external beam radiation therapy. **(B)** Corresponding apparent diffusion coefficient (ADC) image and **(C and D)** 0.16 cc ^{1}H MRSI spectral array. The red arrows on the ADC image indicate a region of clear cut ADC reduction in the right midgland of the prostate ($\leq 1.0 \times 10^{-3}$ mm^2/sec), which was not clear on the corresponding T_2-weighted image (**A**). Spectra overlapping the region of reduced ADC **(C and D)** demonstrated and absence of citrate and polyamines and a very elevated choline to creatine ratio. A subsequent MR targeted TRUS guided biopsy demonstrated a large volume of recurrent Gleason 4+4 cancer in the same location as the ADC and metabolic abnormalities.

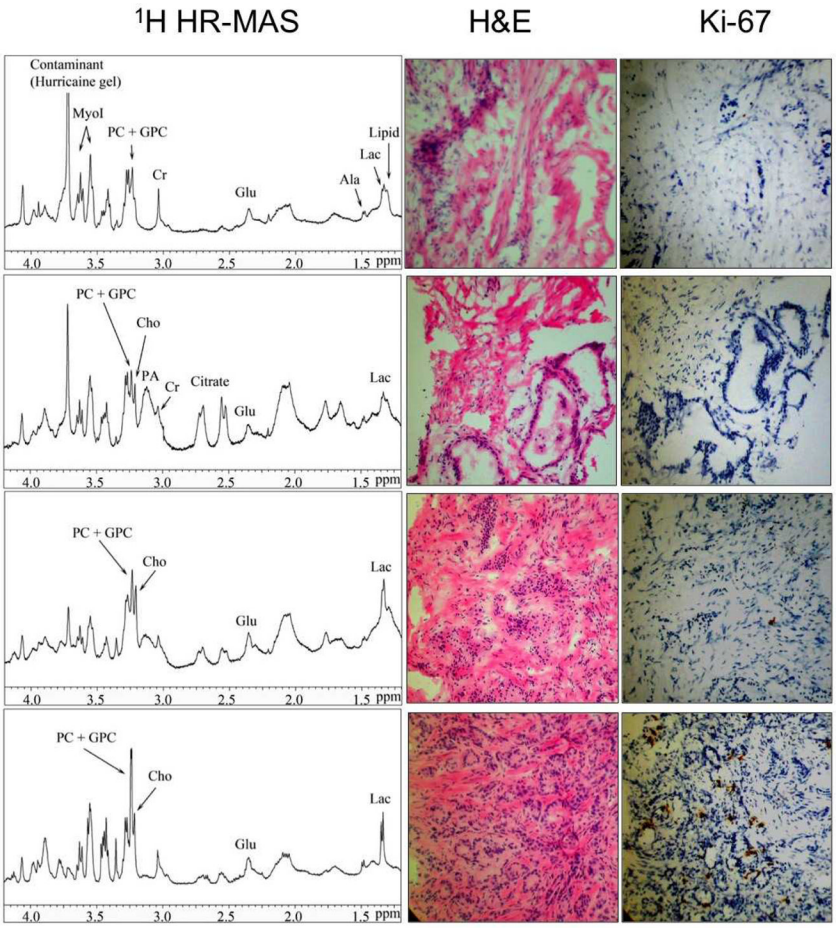

Figure 2.

A comparison of representative 1D HR-MAS spectra, and corresponding H&E and Ki-67-stained sections of snap-frozen prostate biopsy tissues taken from regions of **(A)** benign stromal tissue (5% glandular, 95% stromal, 0% Ki-67), **(B)** benign glandular tissue (38% glandular, 62% stromal, 0% Ki-67), **(C)** indolent cancer (10% Gleason 3+3, 30% glandular, 60% stromal, 1% Ki-67) and **(D)** aggressive prostate cancer (27% Gleason 4+3, 15% glandular, 38% stromal, 13% Ki-67). (Left) One-dimensional HR-MAS spectra. Corresponding hemoatoxylin/eosin (H&E)-stained histologic (middle) and Ki-67-stained sections (right). The major metabolites resonances are shown. PC, phosphocholine; GPC, glycerophosphocholine; Cho, free choline; Cr, creatine; PA, polyamines; MyoI, myo-inositol; Glu, glutamate; Ala, alanine; Lac, lactate;

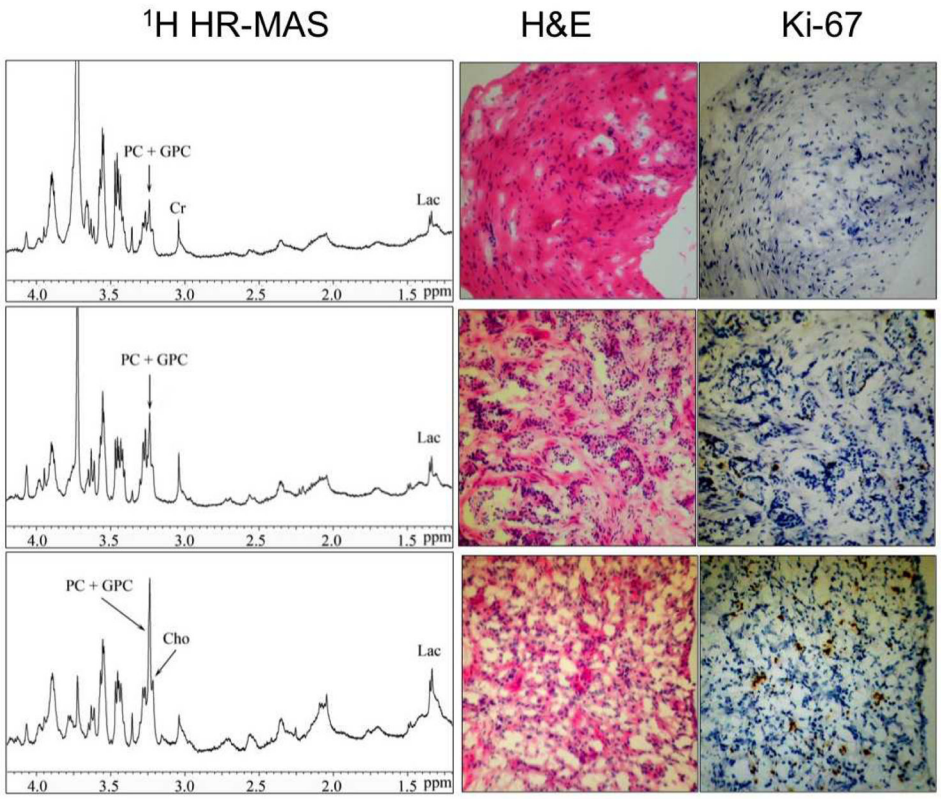

Figure 3.

A comparison of representative 1-D HR-MAS spectra, and corresponding H&E and Ki-67-stained sections of snap-frozen post-radiation prostate biopsy tissues taken from regions of **(A)** residual benign tissue (100% stromal, 0% Ki-67), **(B)** indolent/dying recurrent cancer (45% Gleason 3+4, 5% glandular, 50% stromal, 1% Ki-67) and **(C)** aggressive cancer (42% Gleason 4+3, 5% glandular, 53% stromal, 10% Ki-67). (Left) One-dimensional HR-MAS spectra. Corresponding hemoatoxylin/eosin (H&E)-stained histologic (middle) and Ki-67-stained sections (right).

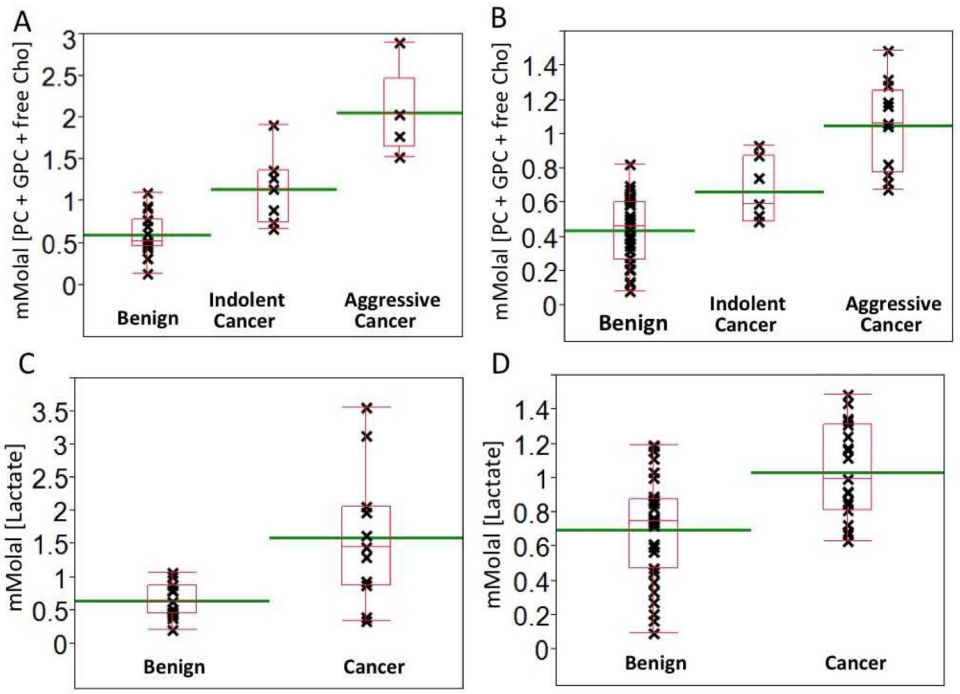

Figure 4.

(A and B) Quantitative comparison of phosphocholine (PC), glycerophosphocholine (GPC) and free choline concentrations in untreated and post-radiation prostate biopsy tissues. In untreated biopsy tissues (left), [PC+GPC] was found to be statistically significant between all three tissue types (benign, indolent and aggressive cancer). In post-radiation biopsy tissues (right), [PC+GPC] was found to be statistically significant between benign and recurrent aggressive cancer, and between recurrent indolent and aggressive cancer). **(C and D)** Quantitative comparison of lactate concentrations in untreated and post-radiation prostate biopsy tissues. [Lactate] was found to be statistically significantly different between benign and malignant biopsy tissue in both untreated and post-radiation biopsy tissues, but did not discriminate between indolent and aggressive cancer.

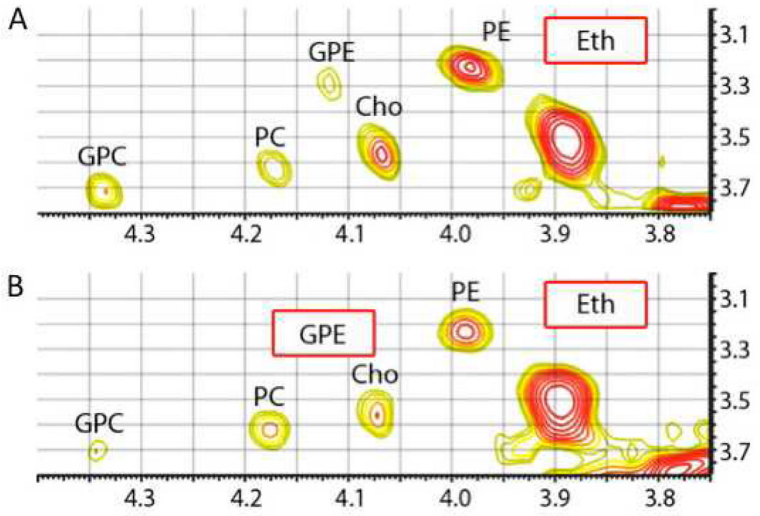

Figure 5.

A comparison of representative 2-D HR-MAS total correlation spectra of snap-frozen prostate biopsy tissues taken from regions of untreated aggressive prostate cancer (27% Gleason 4+3, 15% glandular, 38% stromal, 13% Ki-67) **(A)** and post-radiation aggressive prostate cancer (42% Gleason 4+3, 5% glandular, 53% stromal, 10% Ki-67) **(B)**. The major metabolites resonances are shown. PE, phosphoethanolamine; GPE, glycerophosphoethanolamine; Eth, ethanolamine;

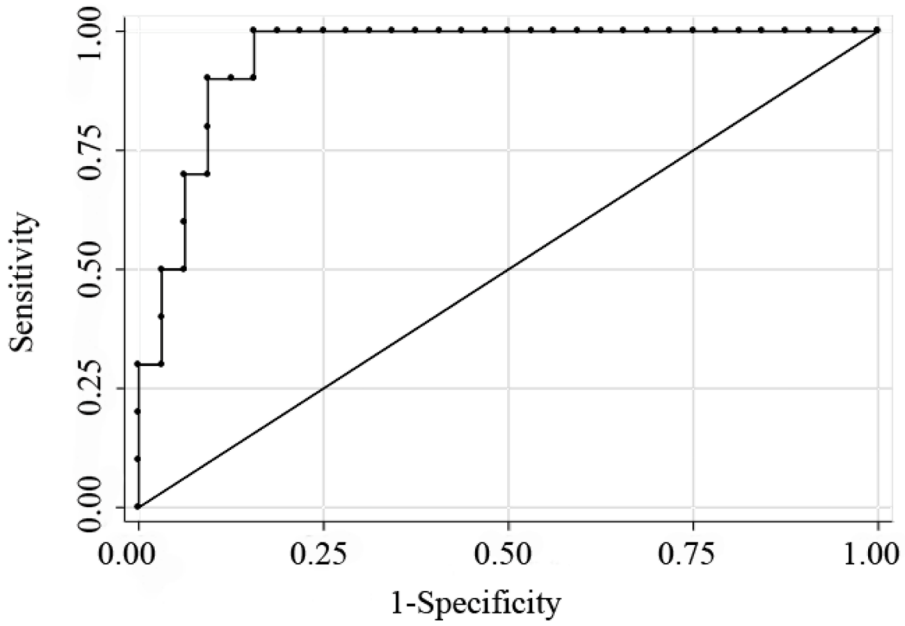

Figure 6.
The performance of using total choline (PC+GPC+Cho) to creatine ratio to diagnose aggressive residual disease was described using receiver operating characteristic (ROC) curve. The area under the ROC curve was 95% (confidence interval = 0.88 to 1.00) indicating that the magnitude of the *in vivo* total choline to creatine ratio would be an accurate predictor of aggressive recurrent prostate cancer after radiation therapy.

Table 1

Patient Characteristics

	Pretreatment patients (n=47)	Post-radiation patients (n=39)
Age (years mean ± SD)	69.3 ± 7.4	68.4 ± 7.0
PSA (ng/ml mean ± SD)	9.8 ± 12.0	2.7 ± 2.1
Type of Radiation therapy		
External beam	-	15
Permanent prostate seed implantation (PPI) brachytherapy	-	17
Combination of external beam and PPI brachytherapy	-	1
High-dose-rate (HDR) brachytherapy		2
Combination of external beam and HDR brachytherapy		2
Proton beam	-	1
Combination of external beam and proton beam	-	1

Table 2

Patient Biopsy Characteristics

	Biopsies obtained pretreatment (n=71)			Biopsies obtained ~6.4 years post-radiation treatment (n=53)		
	Aggressive (n=5)	**Indolent* (n=8)**	**Benign** (n=58)**	**Aggressive (n=12)**	**Indolent* (n=7)**	**Benign (n=34)**
Ki-67 labeling index	10.8 ± 1.7	1.44 ±0.33	0.23 ± 0.14	16.3 ± 3.3	1.00 ± 0.42	0.10 ± 0.09
Gleason score (n)						
3+3	0	7	-	0	3	-
3+4	0	1	-	2	4	-
4+3	3	0	-	2	0	-
≥ 4+4	2	0	-	8	0	-

* The Ki-67 index for indolent cancer was significantly different from aggressive cancer for both untreated and post-radiations biopsy samples.

** The Ki-67 index was not different between untreated predominately glandular and stromal benign biopsy samples.

Table 3

Significant Metabolic Differences Between Benign and Malignant Untreated Prostate Biopsies

Metabolite (mmolal ± SE)	**Benign (n=58)**	**Cancer (n=13)**		***p***
[PC + GPC + free Cho]	0.61 ± 0.05	1.57 ± 0.19		**<0.001**
[PE]	0.78 ± 0.09	1.15 ± 0.17		**0.03**
[lactate]*	0.78 ± 0.16	1.60 ± 0.31		**0.01**
[alanine]	0.27 ± 0.03	0.54 ± 0.05		**<0.001**
[Glutamate]	1.57 ± 0.17	2.62 ± 0.26		**<0.001**
[Citrate]†	6.11 ± 0.75	4.48 ± 0.74		**0.0015**
[Polyamines]†	0.74 ± 0.20	0.35 ± 0.15		**0.0036**
Metabolite (mmolal ± SE)	**Benign** (n=58)	**Indolent Cancer** (n=8)	**Aggressive Cancer** (n=5)	***p***
[PC + GPC + free Cho]	0.61 ± 0.05	1.22 ± 0.19	2.06 ± 0.23	**0.003**[a], **<0.001**[b], **0.02**[c]

*n = 54 for lactate in benign and n = 10 for lactate in cancer biopsy samples.

†Only predominately glandular biopsies (N=38). [Citrate] and [polyamines] were significantly higher in predominantly glandular relative to predominantly stromal benign biopsies ($p \leq 0.001$).

[a]Indolent *versus* benign.

[b]Aggressive *versus* benign.

[c]Indolent *versus* Aggressive.

Table 4

Metabolite Concentrations in Treated Biopsies

Metabolite (mmolal ± SE)	**Benign (n=34)**	**Cancer (n=19)**		**p**
[PC + GPC + free Cho]	0.44 ± 0.03	0.91 ± 0.07		**<0.001**
[Lactate]	0.70 ± 0.05	1.04 ± 0.06		**0.001**
Metabolite (mmolal)	**Benign** (n=34)	**Indolent Cancer** (n=7)	**Aggressive Cancer** (n=12)	**p**
[PC + GPC + free Cho]	0.44 ± 0.03	0.66 ± 0.07	1.05 ± 0.07	0.37[a], **<0.001**[b], **0.04**[c]

[a] Indolent *versus* Benign.

[b] Aggressive *versus* Benign.

[c] Indolent *versus* Aggressive